# Effect of structure, surface passivation, and doping on the electronic properties of Ge nanowires: A first-principles study

D. Medaboina,[1] V. Gade,[1] S. K. R. Patil,[2] and S. V. Khare[3,*]
[1]*Department of Electrical Engineering and Computer Science, The University of Toledo, Toledo, Ohio 43606, USA*
[2]*Department of Mechanical Engineering, The University of Toledo, Toledo, Ohio 43606, USA*
[3]*Department of Physics and Astronomy, The University of Toledo, Toledo, Ohio 43606, USA*
(Received 18 April 2007; revised manuscript received 14 August 2007; published 30 November 2007)

We investigate the structural, energetic, and electronic properties of hydrogen-passivated doped and undoped germanium nanowires along [001], [110], and [111] directions, with diameter $d$ up to 3 nm, using *ab initio* methods. A critical diameter $d_c \approx 2$ nm is found, above which all wires have faceted cross sections determined by the symmetry of their axis. The wires possess several electronic properties relevant for sensing and other nanoelectronic applications: (i) Quantum confinement has a substantial effect on the electronic band structure and, hence, the band gap ($E_g$), which increases with decreasing diameter. (ii) Wires oriented along [110] are found to have a direct $E_g$, while the wires along [111] are found to have an indirect $E_g$. Wires along [001] show a crossover from a direct to an indirect $E_g$ as diameter increases, the value of the critical diameter for the transition being 1.3 nm. (iii) The electronic band structure shows a significant response to changes in surface passivation with hydrogen. (iv) Doping of wires with *n*- and *p*-type atoms produced a response in the band structure similar to that in a doped bulk crystal.

DOI: 10.1103/PhysRevB.76.205327 PACS number(s): 68.55.Jk, 68.65.La, 81.07.Vb, 61.46.−w

## I. INTRODUCTION

A nanowire (NW) is a structure for which two of its dimensions are small (<100 nm), while the third dimension can be as long as a few micrometers. They (NWs) come in different geometric shapes such as wires, tubes, rods, and belts.[1–4] They exhibit many properties and applications very different from their corresponding bulk form. Therefore, they have been assiduously studied recently for their potential applications in electronic devices and sensors.[5–14] NWs were found to exhibit a quantum confinement effect in the direction perpendicular to the growth direction and periodic band structures in the direction parallel to the direction of growth.[15] Due to the wide adjustability of NW optoelectronic properties, their use in photovoltaic cells, photodetectors, field effect transistors, and other devices has been investigated.[16,17]

Many materials have been used for the generation of NWs.[11,12,14,18] Of more specific experimental interest have been the NWs made of Si due to the ease of integrating them into devices with current Si infrastructure.[19–21] Several computational studies, using *ab initio* methods, of structure-property relationship in Si NWs have also been carried out.[22–25] These studies involved the structural, energetic, electronic, and optical properties of hydrogen- and halogen-passivated silicon nanowires along [001], [110], [111], and [112] orientations, using different forms of first-principles approaches. Some of them computed band gaps and dielectric constants comparable to those found in experiments, with GW[23] or screened exchange[24] approximations. Quantum confinement effects were found for nanowire diameters below ≈2.0 nm. It was concluded that surface passivation of Si dangling bonds, by different chemical species and with different surface concentrations, and also doping by *p*- or *n*-type atoms have a strong effect on the band structure and band gaps.[15,23] Collectively these results suggest that Si NWs are good candidates for sensing and optical applications.

It is well known that Ge has many advantages over Si for electronic applications.[10,26] Therefore, significant experimental investigations of Ge NWs have been reported recently.[5–14] Wang *et al.*[14] synthesized Ge nanowires experimentally using chemical vapor deposition and examined the surface chemistry and electrical properties of Ge nanowires with *p* and *n* dopants. They observed opposite band bending in *n*- and *p*-type doped nanowires due to changes in the resulting surface passivation. Mathur *et al.*[11] synthesized Ge nanowires using laser ablation and chemical vapor transport reactions at higher temperatures. They observed a low field shift in the Raman spectra (RS) of Ge NWs, compared to bulk, due to strain caused by dimensional confinement. Sun *et al.*[12] synthesized Ge NWs with diameters from about 30 nm to tens of micrometers, using thermal evaporation of Ge powder. They observed NWs having a diamond structure and observed [111] as the preferred growth direction. Kamanev *et al.*[13] concluded from differences in the RS and photoluminescence spectra of Ge NWs grown on Si(001) and Si(111) that wires grown on the former surface were relaxed, while those on the latter showed Si-Ge intermixing and strain.

Motivated by this recent interest in experimental and theoretical studies[27–29] we focus here on the theoretical study of structural, energetic, and electronic properties of hydrogen-passivated Ge NWs, using first-principles calculations, varying the (i) wire diameter, (ii) orientation of axis, (iii) concentration of passivating H atoms at the surface, and (iv) the presence of *n*- and *p*-type dopant atoms.

## II. *AB INITIO* METHOD

Our calculations were performed in the framework of density functional theory,[30] within the local density approximation (LDA) using VASP.[31–35] Core electrons were implicitly treated by ultrasoft Vanderbilt pseudopotentials.[36,37] For

 

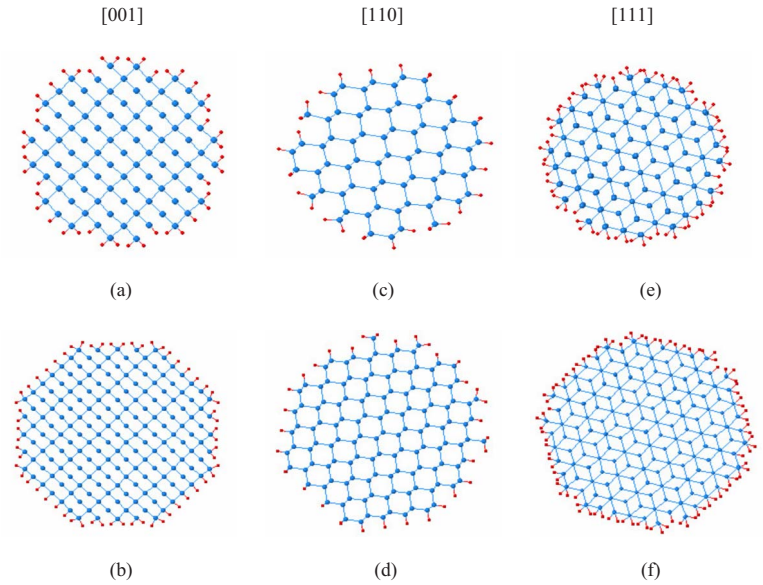


FIG. 1. (Color online) Cross-sectional views of the relaxed Ge NWs. (a) $NW_{[001]}^{(Ge-89,H-44)}(2.03)$, (b) $NW_{[001]}^{(Ge-185,H-60)}(3.03)$, (c) $NW_{[110]}^{(Ge-69,H-32)}(2.12)$, (d) $NW_{[110]}^{(Ge-133,H-40)}(3.3)$, (e) $NW_{[111]}^{(Ge-170,H-66)}(2.11)$, and (f) $NW_{[111]}^{(Ge-326,H-90)}(3.03)$. Larger blue circles represent Ge atoms and the smaller red ones represent the H atoms used to saturate dangling bonds. Local geometrical patterns corresponding to the axis of the wires are evident: square shapes for [001] axis, hexagonal for [110], and parallelograms for [111].

each calculation, irreducible $k$ points were generated using the Monkhorst-Pack sampling scheme,[38] with a sufficient number of $k$ points as determined by convergence tests. These tests have shown that $k$-point grids from $2\times2\times6$ to $2\times2\times18$ gave sufficient accuracy in the calculation of total energies and forces, depending on the supercell shape and size. The single-particle wave functions were expanded in a plane-wave basis using a 150 eV kinetic energy cutoff, which was determined by convergence tests to be sufficient. As a test of the pseudopotentials used, we computed for bulk

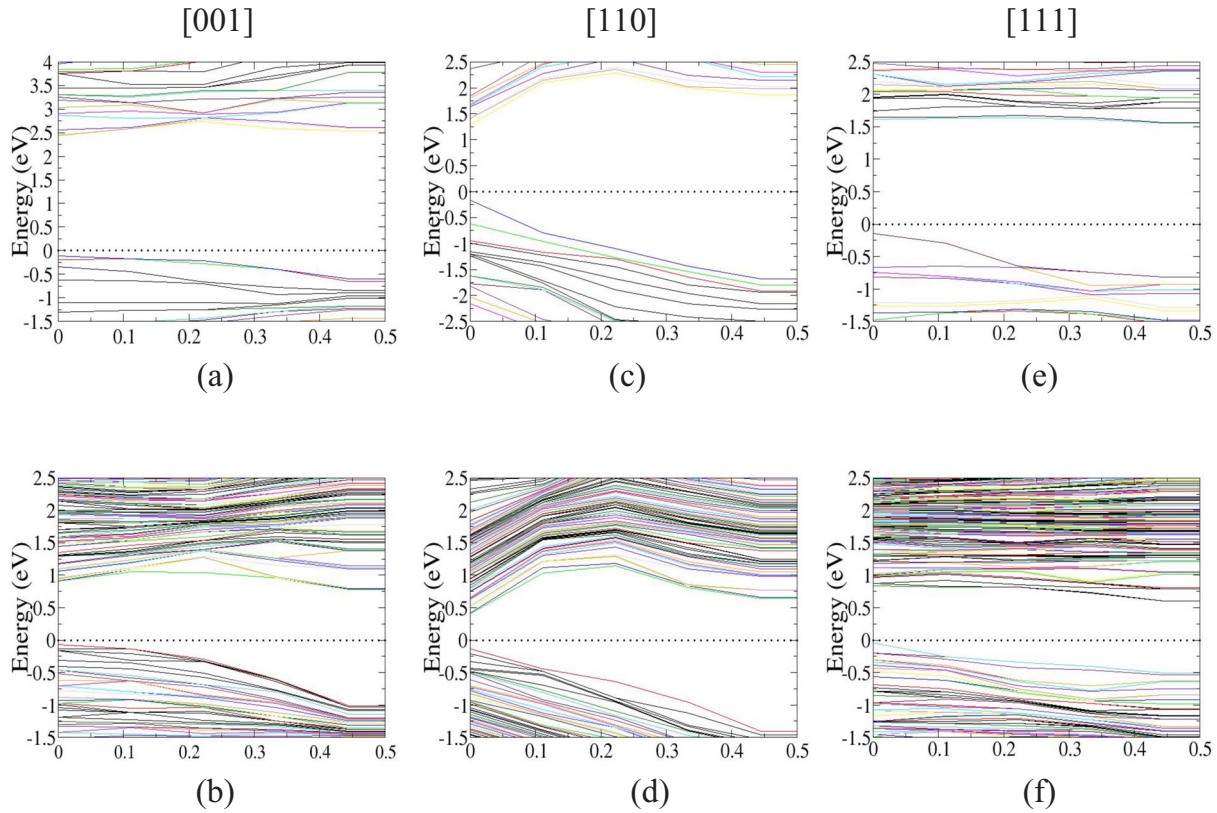


FIG. 2. (Color online) Band structure of Ge NW along [001], [110], and [111] directions. The Fermi level in each panel is set to zero and is shown by the dotted line. (a) $NW_{[001]}^{(Ge-25,H-20)}(1.12)$ and (b) $NW_{[001]}^{(Ge-185,H-60)}(3.03)$ represent the band structure along the [001] direction. (c) $NW_{[110]}^{(Ge-17,H-12)}(1.12)$ and (d) $NW_{[110]}^{(Ge-133,H-40)}(3.3)$ represent the band structure along the [110] direction. (e) $NW_{[111]}^{(Ge-62,H-42)}(1.23)$ and (f) $NW_{[111]}^{(Ge-326,H-90)}(3.03)$ represent the band structure along the [111] direction.

Ge a lattice constant of 0.5638 nm and a bulk modulus of 72.57 GPa, in excellent agreement with experimental values[39] of 0.5658 nm and 75 GPa, respectively. The theoretical lattice constant was used in all calculations.

## III. NANOWIRE STRUCTURE

We have studied different geometries of Ge NWs along [001], [110], and [111] crystallographic directions of the diamond lattice. We started with wires which were bulk terminated and had circular cross sections. All dangling bonds on the surface were saturated with hydrogen (H) atoms. This procedure is known to remove surface states from the band gap ($E_g$) of the material. The typical Ge-H bond length was around 0.15 nm, and varied around this value depending on the local geometry of the surface.

The smallest repeating unit along the wire axis was used to create an effectively infinite wire by periodic repetition of this unit along the wire axis. This was taken to be the $Z$ axis. Two directions perpendicular to the wire axis were taken as the $X$ and $Y$ axes, and a tetragonal supercell with a large vacuum region was used. Typical center to center distance between two periodically repeating wires was ($d$+0.6 nm) along the $X$ and $Y$ axes, where $d$ was the diameter of the wire. This large vacuum ensured that there was negligible interaction between wires. The atomic positions of all atoms were then fully relaxed using the first-principles methods described above. Energy convergence to better than 1 meV was obtained in the fully relaxed structures.

## IV. RESULTS

More than 30 wires constructed along the three axes ([001], [110], and [111]), of different diameters up to 3 nm, were fully relaxed. Figure 1 shows the structures of some of these different NWs. The compact notation $\mathrm{NW}_{[hkl]}^{(\mathrm{Ge}-m,\mathrm{H}-n,\ldots)}$(d) represents a NW along an axis of Miller indices [$hkl$] containing $m$ Ge and $n$ H atoms, with additional entries for more elements as needed, with a diameter $d$ expressed in nanometers. As an example, $\mathrm{NW}_{[001]}^{(\mathrm{Ge}-89,\mathrm{H}-44)}(2.03)$ represents a NW along the [001] axis containing 89 Ge atoms and 44 H atoms, with a diameter of 2.03 nm. To represent a doped nanowire, we have the third element in the superscript to signify the type and number of dopant atoms. The optimized structures of NWs are highly symmetric and, in general, lack significant surface reconstruction due to the passivation of the dangling bonds by H. Figure 1 shows that surface atoms of the NWs relax more than atoms nearer to the center. It was observed that bond lengths between Ge atoms at the surface were relaxed by ≈1%, whereas no relaxation was observed for atoms in the interior region away from the surface. When the NWs were allowed to dimerize, it was observed that atoms relaxed by ≈50% as expected. Cross sections of wires along [110] were found to have cylindrical structures for all diameters. Along [001] and [111] axes, the smaller wires with diameters $d<d_c$ have circular cross sections. As seen from Fig. 1, the critical diameter $d_c$ above which the cross section acquires a faceted shape lies in the range 2.0 nm $<d_c<$3.0 nm for these ([001] and [111]) axes. The value of $d_c$ is determined by the competition to lower the total energy, between energies of the different exposed surfaces of H terminated Ge, under the constraint of a fixed volume. Wires along the [001] direction appear in Fig. 1 to have a rectangular bonding geometry rather than the expected square surface arrangement of atoms in a single (001) surface layer. This expected square arrangement of atoms of a diamond lattice is not made of nearest neighbor atoms. The rectangular structure seen in Fig. 1 arises because the middle atoms, along the longer side of the rectangle, are nearest neighbors of the top layer atoms and are one layer below the top layer. For bigger diameter ($d>d_c$=2.15 nm) wires along [001], cross sections were found to be octagonal shaped with facets

TABLE I. The band gaps $E_g$ of various Ge NWs oriented along different axes and having different diameters, and hence, different number of atoms. The nature of the band gap, (D) for direct and (I) for indirect is also shown. All direct $E_g$ occur at the Γ point. All indirect $E_g$ occur with the VB maximum at Γ point (0,0,0) and the CB minimum at $(0,0,(0.88\pi)/d_r)$.

| Wire axis [$hkl$] | $d$ (nm) | No. of Ge atoms | No. of H atoms | $E_g$ (eV) | Type of band gap |
|---|---|---|---|---|---|
| [001] | 0.41 | 5 | 12 | 4.30 | D |
| | 0.57 | 9 | 12 | 3.90 | D |
| | 0.82 | 13 | 20 | 3.05 | D |
| | 1.12 | 25 | 20 | 2.53 | D |
| | 2.03 | 89 | 44 | 1.3 | I |
| | 3.03 | 185 | 60 | 0.85 | I |
| [110] | 0.80 | 10 | 16 | 2.04 | D |
| | 1.12 | 17 | 12 | 1.42 | D |
| | 2.12 | 69 | 32 | 0.78 | D |
| | 3.3 | 133 | 40 | 0.53 | D |
| [111] | 0.46 | 14 | 18 | 3.25 | I |
| | 0.80 | 26 | 30 | 2.58 | I |
| | 1.42 | 62 | 42 | 1.70 | I |
| | 2.11 | 170 | 66 | 0.95 | I |
| | 3.02 | 326 | 90 | 0.64 | I |

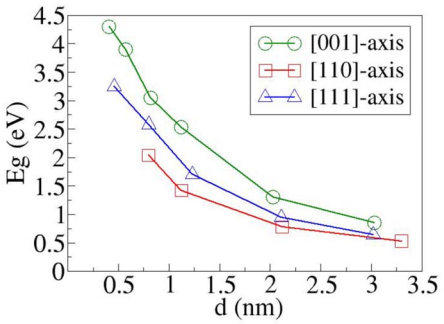


FIG. 3. (Color online) Plot of $E_g$ versus diameter for various axis of orientation.

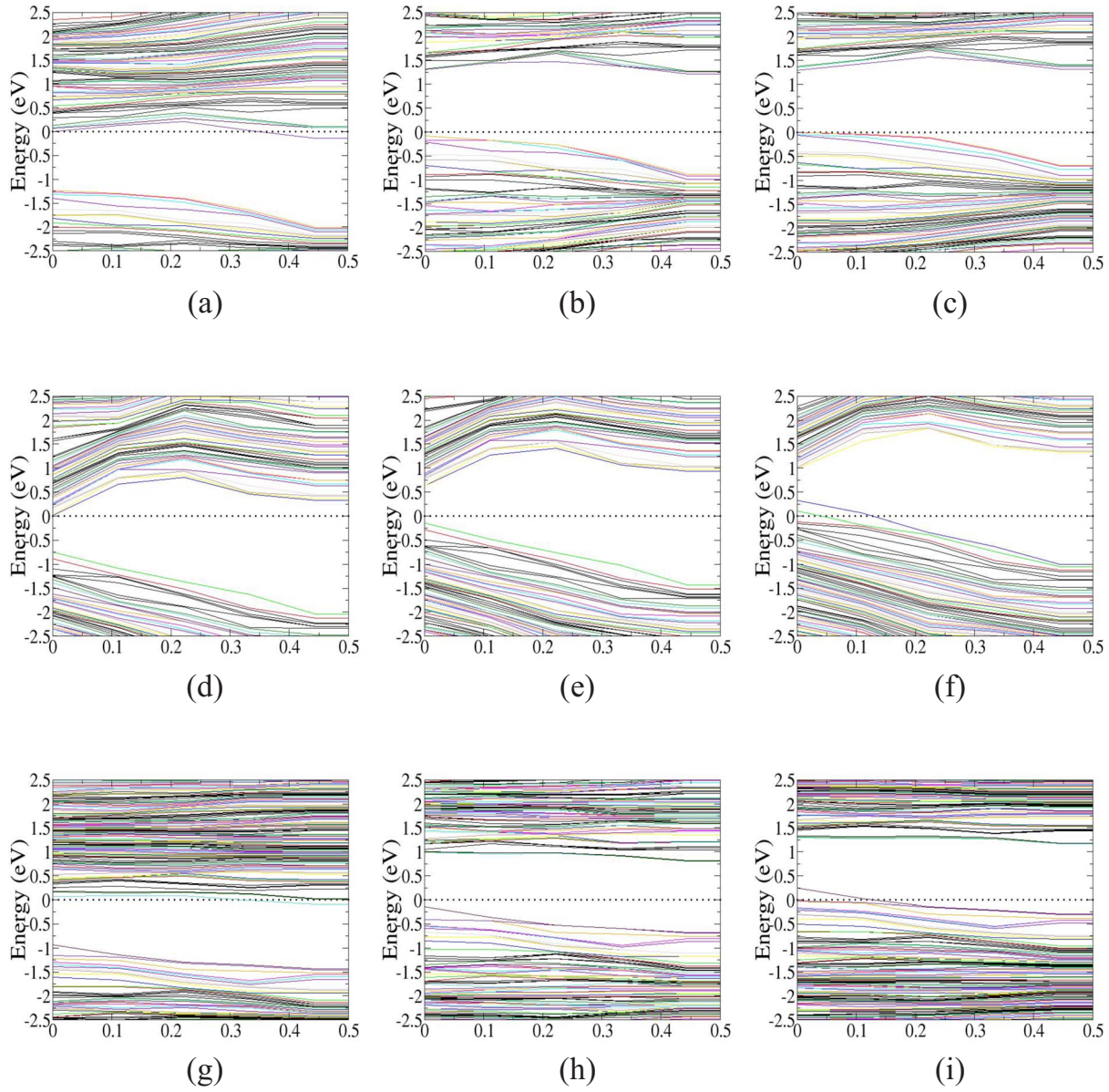


FIG. 4. (Color online) Comparison of band structures of Ge NWs with and without doping. The Fermi level in each panel is set to zero and is shown by the dotted line. (a) $NW_{[001]}^{(Ge-88,H-44,P-1)}(2.03)$, (d) $NW_{[110]}^{(Ge-68,H-32,P-1)}(2.12)$, and (g) $NW_{[111]}^{(Ge-169,H-66,P-1)}(2.11)$ are *n*-type doped wires. (b) $NW_{[001]}^{(Ge-89,H-44)}(2.03)$, (e) $NW_{[110]}^{(Ge-69,H-32)}(2.12)$, and (h) $NW_{[111]}^{(Ge-170,H-66)}(2.11)$ are undoped wires. (c) $NW_{[001]}^{(Ge-88,H-44,B-1)}(2.03)$, (f) $NW_{[110]}^{(Ge-68,H-32,B-1)}(2.12)$, and (i) $NW_{[111]}^{(Ge-169,H-66,B-1)}(2.11)$ are *p*-type doped wires.

of the {001} and {110} type, which were normal to [001]. For bigger diameter ($d > d_c = 2.11$ nm) wires along [111], they were hexagonal shaped with facets of the {110} type, which were normal to [111]. We also observed that due to the differing atomic densities in different planes, for a fixed diameter, wires oriented along the [111] direction have a larger number of atoms compared to wires along the [001] direction, which, in turn, have a larger number of atoms compared to wires along [110]. Surface energies were calculated for our NWs, and were found to be linearly dependent on $d$. These surface energies[40] were found to be approximately in the ratio 4:5:3, respectively, for wires along [001], [110], and [111], reflecting the relative energy contributions of the exposed facets to the total energy of the NW. We also found that the energy per Ge atom in any NW decreases with increasing diameter and approaches the energy of the bulk per Ge atom.

Electronic band structures of the relaxed wires were calculated from $\Gamma$ (0,0,0) point to $X$ $(0,0,2\pi/d_r)$ along the wire axis, where $d_r$ is the length of the repeating unit of the wire along its axis. Figure 2 shows the band structures for the wires over half this range[41] for the wires shown in Fig. 1. We observed that the dispersion of the valence band (VB) for wires with approximately the same diameter is greatest for wires along [110] and least for wires along [111]. As expected from a quantum size effect, we observed that the ab-

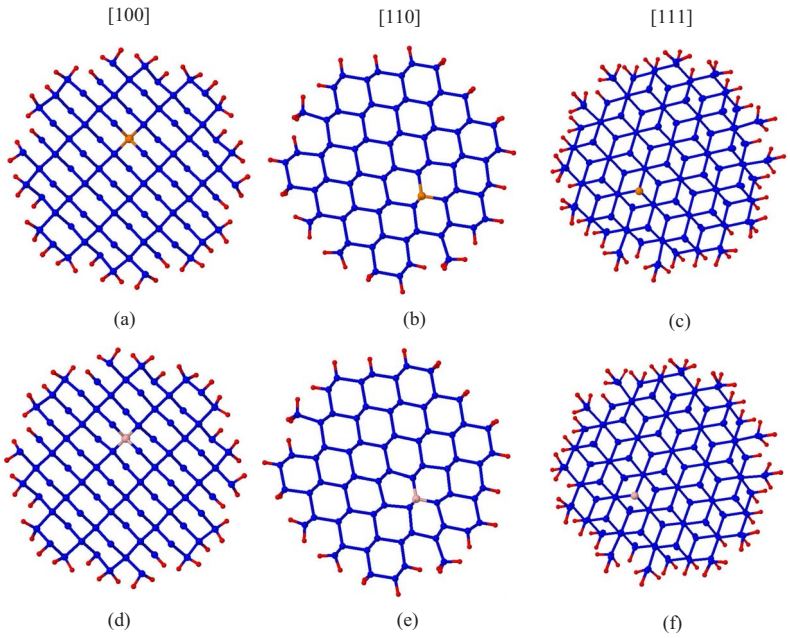


FIG. 5. (Color online) Cross-sectional views of the relaxed doped Ge NWs. (a) $NW_{[001]}^{(Ge-88,H-44,P-1)}(2.03)$, (d) $NW_{[001]}^{(Ge-88,H-44,B-1)}(2.03)$, (b) $NW_{[110]}^{(Ge-68,H-32,P-1)} \times (2.12)$, (e) $NW_{[110]}^{(Ge-68,H-32,B-1)}(2.12)$, (c) $NW_{[111]}^{(Ge-169,H-66,P-1)}(2.11)$, and (f) $NW_{[111]}^{(Ge-169,H-66,B-1)}(2.11)$. Larger blue circles represent Ge atoms, orange circles [in (a)–(c)] represent phosphorus atoms, brown circles [in (d)–(f)] represent boron atoms, and the smaller red ones represent the H atoms used to saturate dangling bonds.

solute value of the VB maximum decreases in energy and the absolute value of the conduction band (CB) minimum increases in energy as the thickness of the wire decreases. This effect of quantum confinement of electrons is easily observed in the range of diameters we studied. This leads to an increase in the electronic $E_g$ with decreasing NW diameter. Similar results have been obtained in other studies, especially for Si NWs.[15,23,42] Table I displays a sampling of these values of $E_g$. These data show that NW $E_g$ could be either direct or indirect, depending on the crystallographic orientation. NWs along [110] and thin ($d \leqslant 1.3$ nm) ones along [001] have direct band gaps occurring at the $\Gamma$ point. Such wires, due to their direct gaps, would be suitable for applications in optics. Wires along [001] were found to transit from direct to indirect $E_g$ as the diameter increased above 1.3 nm, while all wires along [111] have indirect band gaps. Kholod *et al.*,[43] have made similar observations when they studied unrelaxed Ge quantum wires along (100), (110), and (111) axes. Figure 3 shows the plot of $E_g$ versus $d$, which clearly depicts that the $E_g$ depends on both the thickness of the wire and its orientation. Among the band structures we calculated the largest $E_g \approx 4.3$ eV, within LDA, was found for $NW_{[001]}^{(Ge-5,H-12)}(0.41)$. We observed for wires with the same diameter but different orientations that $E_g$ is greatest for wires along [001] and lowest for wires along [110]. For comparison, for our pseudopotentials we found that the $E_g$ for bulk Ge between the $\Gamma$ and $L$ $k$ points was 0.06 eV and the direct $E_g$ at $\Gamma$ was 0 eV. These values may be attributed to the manner in which semicore states of Ge are treated as commented by Tiago *et al.*[44] and Beckman *et al.*[45]

There are distinct differences in the behavior of $E_g$ for NWs of Ge compared to those of Si, as seen from earlier computations.[15,23] For Si, NWs along [110] and thin ($d \leqslant 2.2$ nm) NWs along [111] have direct band gaps occurring at the $\Gamma$ point. It has also been shown[23] that Si NWs along [111] have a greater $E_g$ than those along [110] with the same diameter. These differences in the variation of the band gaps of NWs, from direct to indirect, with orientation and diameter can be attributed to differences in the location of the conduction band minima of the two materials. Si has six ellipsoidal conduction bands with axes along the $\langle 001 \rangle$ directions, while Ge has eight ellipsoidal conduction bands along the $\langle 111 \rangle$ axes.

Besides this dependence of $E_g$ on $d$ and the orientation of the growth axis, other ways for modifying the electronic properties would be important for applications. Surface adsorption and doping are two ways in which this may be achieved. NWs have already been contemplated as the active elements in sensing devices because the large surface area is believed to cause the sensitive dependence of electronic properties on changes in surface adsorption by different chemical species.[9] To demonstrate this effect in a simple model system, we also studied the electronic structures of NWs along [111], which have facets of {110} and {100} types, by changing the surface hydrogen concentration. This orientation was chosen because of the tendency of the unhydrogenated facets to dimerize. Hydrogen atoms were removed from the surface of relaxed wires. Band structures of these wires were found to have electronic states with energies lying in the middle of $E_g$ due to the occurrence of unpaired electrons on the surface of the NW after the removal of H atoms. This change in the electronic properties with a change in hydrogen concentration for wires along [111] could be potentially exploited in sensing applications, due to the disappearance of the $E_g$, which would cause a significant increase in electronic conduction. Similar results for Si NWs have been observed in other computations.[15,23]

Band bending caused by doping Ge NWs has been demonstrated experimentally.[9] Motivated by this result, we doped our NWs with boron and phosphorus. Highly doped $p$-type ($n$-type) wires are obtained by the addition of a boron (phosphorus) atom in the interior of the NW. Doping was performed for NWs of $d \approx 2.0$ nm along each axis. The concentration of dopants was very high such as one dopant for 89 Ge atoms in the unit cell along the [001] axis, one dopant for

69 atoms along the [011] axis, and one dopant for 170 Ge atoms along the [111] direction. These structures were allowed to relax, and their band structures were studied subsequently. Cross-sectional views of these relaxed doped Ge NWs are shown in Fig. 4.

Figure 5 shows the band structures of doped Ge NWs for a single wire along each crystallographic direction ([001], [110], and [111]). A high level of doping (0.5–1.5%) obviously has an impact on the electronic structures of Ge NWs. As shown in Fig. 5, adding a *p*-type (*n*-type) dopant moves the $E_F$ toward the VB (CB). The maximum of the VB and the minimum of the CB increase (decrease) in energy with the addition of *p*-type (*n*-type) dopant when measured relative to $E_F$. Figure 5 also shows that the doping of wires does not have a significant effect on the dispersion of VB and CB. Thus, the effect of doping on the band structure of hydrogenated Ge NWs is similar to that in doped bulk Ge. This property would make Ge NWs suitable for applications which require the tuning of the NW conductivity by doping.

## V. CONCLUSIONS

We have studied from first principles the structural, electronic, and energetic properties of doped and undoped Ge NWs along three principal growth directions [001], [110], and [111]. The NW growth direction and diameter have a significant effect on the structural and electronic properties. Wires above a certain critical diameter $d_c \approx 2$ nm begin to show faceting of their surfaces, due to the orientation dependence of the surface energies of the exposed Ge facets. The electronic band structures and band gaps show a significant dependence on the diameter, NW axis orientation, surface passivation, and doping. We show that a change in the surface passivation of dangling bonds produces a substantial effect on the NW electronic structure. This sensitive response could be beneficial in a variety of sensing and nanoelectronics applications.

## ACKNOWLEDGMENTS

We gratefully thank DARPA (Grant No. HR0011-07-1-0003) for financial support and the Ohio Supercomputing Center and the National Center for Supercomputing Applications for computing resources. We would like to thank Paul W. Leu for help with computation.

*Corresponding author. khare@physics.utoledo.edu

[1] A. Kolmakov and M. Moskovits, Annu. Rev. Mater. Res. **34**, 151 (2004).
[2] M. Law, J. Goldberger, and P. Yang, Annu. Rev. Mater. Res. **34**, 83 (2004).
[3] Y. Xia, P. Yang, Y. Sun, Y. Wu, B. Mayers, B. Gates, Y. Yin, F. Kim, and H. Yan, Adv. Mater. (Weinheim, Ger.) **15**, 353 (2003).
[4] O. Masala and R. Shesadri, Annu. Rev. Mater. Res. **34**, 41 (2004).
[5] Y. Wu and P. Yang, Chem. Mater. **12**, 605 (2000).
[6] Y. Wu, R. Fan, and P. Yang, Nano Lett. **2**, 83 (2002).
[7] L. J. Lauhon, M. S. Gudiksen, D. Wang, and C. M. Lieber, Nature (London) **420**, 57 (2002).
[8] T. Hanrath and B. A. Korgel, Small **1**, 717 (2005).
[9] D. Wang and H. Dai, Appl. Phys. A: Mater. Sci. Process. **85**, 217 (2006).
[10] P. Nguyen, H. T. Ng, and M. Meyyappan, Adv. Mater. (Weinheim, Ger.) **17**, 549 (2005).
[11] S. Mathur, H. Shen, V. Sivakov, and U. Werner, Chem. Mater. **16**, 2449 (2004).
[12] X. H. Sun, C. Didychuk, T. K. Sham, and N. B. Wong, Nanotechnology **17**, 2925 (2006).
[13] B. V. Kamenev, V. Sharma, L. Tsybeskov, and T. I. Kamins, Phys. Status Solidi A **202**, 2753 (2005).
[14] D. Wang, Y. L. Chang, Q. Wang, J. Cao, D. B. Farmer, R. G. Gordon, and H. Dai, J. Am. Chem. Soc. **126**, 11602 (2004); G. Liang, D. Kienle, S. K. R. Patil, J. Wang, A. W. Ghosh, and S. V. Khare, IEEE Trans. Nanotechnol. **6**, 2 (2007).
[15] A. K. Singh, V. Kumar, R. Note, and Y. Kawazoe, Nano Lett. **6**, 920 (2006).
[16] Y. Cui, Z. Zhong, D. Wang, W. U. Wang, and C. M. Lieber, Nano Lett. **3**, 149 (2003).
[17] X. Duan, Y. Huang, Y. Cui, J. Wang, and C. M. Lieber, Nature (London) **409**, 66 (2001).
[18] P. V. Radovanovic, C. J. Barrelet, S. Gradecak, F. Qian, and C. M. Liber, Nano Lett. **5**, 1407 (2005).
[19] K. Peng, J. Hu, Y. Yan, Y. Wu, H. Fang, Y. Xu, S. T. Lee, and J. Zhu, Adv. Funct. Mater. **16**, 387 (2006).
[20] T. Baron, M. Gordon, F. Dhalluin, C. Ternon, P. Ferret, and P. Gentile, Appl. Phys. Lett. **89**, 233111 (2006).
[21] V. Schmidt, S. Senz, and U. Gosele, Nano Lett. **5**, 931 (2005).
[22] D. D. D. Ma, C. S. Lee, F. C. K. Au, S. Y. Tong, and S. T. Lee, Science **299**, 1874 (2003).
[23] X. Zhao, C. M. Wei, L. Yang, and M. Y. Chou, Phys. Rev. Lett. **92**, 236805 (2004); F. Bruneval, S. Botti, and L. Reining, *ibid.* **94**, 219701 (2005); X. Zhao, C. M. Wei, L. Yang, and M. Y. Chou, *ibid.* **94**, 219702 (2005).
[24] J. Li and A. J. Freeman, Phys. Rev. B **74**, 075333 (2006).
[25] P. W. Leu, B. Shan, and K. Cho, Phys. Rev. B **73**, 195320 (2006).
[26] Ge has higher electron and hole intrinsic mobilities at room temperature, enabling higher frequency devices and faster switching between states, a larger bulk excitonic Bohr radius leading to stronger quantum confinement effects, and also a lattice match with III-V materials like GaAs (Ref. 10).
[27] R. Kagimura, R. W. Nunes, and H. Chacham, Phys. Rev. Lett. **98**, 026801 (2007).
[28] R. N. Musin and X. Q. Wang, Phys. Rev. B **71**, 155318 (2005).
[29] R. Kagimura, R. W. Nunes, and H. Chacham, Phys. Rev. Lett. **95**, 115502 (2005).
[30] W. Kohn and L. J. Sham, Phys. Rev. **140**, A1133 (1965).
[31] http://cms.mpi.univie.ac.at/vasp
[32] G. Kresse and J. Hafner, Phys. Rev. B **47**, 558 (1993).
[33] G. Kresse, thesis, Technische Universität Wien, 1993.
[34] G. Kresse and J. Furthmüller, Comput. Mater. Sci. **6**, 15 (1996).

[35] G. Kresse and J. Furthmüller, Phys. Rev. B **54**, 11169 (1996).
[36] D. Vanderbilt, Phys. Rev. B **41**, 7892 (1990).
[37] G. Kresse and J. Hafner, J. Phys.: Condens. Matter **6**, 8245 (1994).
[38] H. J. Monkhorst and J. D. Pack, Phys. Rev. B **13**, 5188 (1976).
[39] C. Kittel, *Introduction to Solid State Physics*, 2nd ed. (Wiley, New York, 1976), p. 40.
[40] Surface energies were calculated by subtracting $N$ times the energy of a single Ge atom in bulk from the energy of an $N$ atom NW.
[41] By symmetry, we obtain an identical plot for the other range $(0,0,\pi/d_r)$ to $(0,0,2\pi/d_r)$.
[42] M. Bruno, M. Palummo, R. Del Sole, V. Olevano, A. N. Kholod, and S. Ossicini, Phys. Rev. B **72**, 153310 (2005).
[43] A. N. Kholod, V. L. Shaposhnikov, N. Sobolev, V. E. Borisenko, F. A. D'Avitaya, and S. Ossicini, Phys. Rev. B **70**, 035317 (2004).
[44] M. L. Tiago, S. Ismail-Beigi, and S. G. Louie, Phys. Rev. B **69**, 125212 (2004).
[45] S. P. Beckman, J. Han, and J. R. Chelikowsky, Phys. Rev. B **74**, 165314 (2006).